Nanostructural study of sol-gel-derived zirconium oxides

María C. Caracoche, Patricia C. Rivas, and Mario M. Cervera
Departamento de Física, FCE, Universidad Nacional de La Plata, 1900 La Plata, Argentina

Ricardo Caruso, Edgardo Benavídez, Oscar de Sanctis
Laboratorio de Materiales Cerámicos, FCEIA, IFIR, UNR, 2000 Rosario, Argentina

Sergio R. Mintzer
Departamento de Materiales, Gerencia de Desarrollo, Comisión Nacional de Energía Atómica, 1429 Buenos Aires, Argentina

(Received 19 June 2002; accepted 28 October 2002)

Two sol-gel derived zirconia powders were prepared at pH = 0.5 and pH = 5.5. They were investigated as a function of temperature using mainly perturbed angular correlation spectroscopy. The aim was to elucidate the relationship between the nanoscopic configurations around Zr^{4+} ions and the morphology and structure of the powders. The highly porous material resulting from the solution at higher pH could be described mainly by defective and disordered, very hydrolyzed tetragonal arrays. As temperature increased, the amount of these arrays decreased while they became increasingly asymmetric, thus suggesting their superficial localization. The easy removal of hydroxyls led to the early appearance of the monoclinic phase. The gel obtained from the precursor at pH = 0.5 was entirely described by configurations still involving organic residues. After their calcination, the powder underwent a well-defined two-step hydroxyl removal thermal process leading to the crystallization of the tetragonal and the monoclinic phases. The thermal stability of the metastable tetragonal phase in the investigated powders seems to be controlled by their different capability to absorb oxygen.

I. INTRODUCTION

Zirconia-based ceramics have gained recent attention as engineering materials because of their diverse commercial applications. Research on the metastable phases of these materials and their transitions have been a subject of great scientific and technological importance during recent decades. A number of explanations have been offered for the interpretation of the presence of metastable tetragonal as well as cubic zirconia structures at low temperature. Garvie attributed it to crystallite size effects,[1] Wu *et al.* to strain and lattice defects,[2] and other authors to the existence of a certain number of oxygen anion vacancies.[3]

Precipitation and sol-gel methods are the most-used chemical methods to prepare zirconia-based ceramics.[4,5] Although at first sight both methods are similar, the molecular structure configurations of the resulting zirconia precursor gels obtained through them are not. The precipitation-derived product is indeed more hydrous, and consequently, its complex molecular structure contains varying amounts of water in the form of hydrous oxide $ZrO_2 \cdot H_2O$, metazirconic acid H_2ZrO_3, or zirconyl hydroxide $ZrO(OH)_2$. Furthermore, it exhibits a tendency to polymerize. On the other hand, the product obtained by the sol-gel method consists of randomly arranged discrete nanoscopic sol particles with voids within them. It is also known that the resulting molecular structure configuration is strongly dependent on processing parameters such as the type of zirconium alkoxide precursor,[6] the type of the alcoholic solvent,[7] and the pH.[8] In turn, it has been reported that the molecular structure configuration of the precursors strongly affects the crystallization behavior of zirconia.[9] Therefore, crystallization features observed in hydrous zirconias obtained by precipitation might be different from those in sol-gel-derived zirconias.

Many studies have shown that in precipitation-derived zirconia products the precursor solution pH has a marked influence on polymorphic phase formation and also on crystallite growth and thermal transformations. Crystallite size and phase structure have been investigated as a function of the precursor solution pH in gels precipitated from zirconyl chloride,[9] zirconyl nitrate,[10] and zirconium alkoxides,[11] but the role of this factor in sol-gel-derived zirconias has not been elucidated yet.

The aim of this investigation was thus to focus attention to the effects of the starting solution pH on some features of zirconia powders obtained by sol-gel, i.e., the morphology, polymorphic phase content, and involved nanostructures, and also the thermal transformations and

crystallite size evolution. For this purpose, we studied two sol-gel-derived zirconias resulting from precursor solutions of different pHs and their thermal evolution by using the highly localized perturbed angular correlation (PAC) spectroscopy technique and the complementary bulk techniques of x-ray diffraction (XRD), differential thermal analysis and thermogravimetric analysis (DTA-TGA), and specific surface area measurements [nitrogen adsorption Brunauer–Emmett–Teller (BET) method]. Zirconia ceramics are extremely suitable for the application of the PAC technique since natural zirconium contains 1–5% of the hafnium impurities at zirconium sites, and radioactive ^{181}Hf is one of the most efficient PAC probes. Under neutron irradiation of the material under certain conditions, the desired ^{181}Hf activity can be obtained. PAC spectroscopy has been outlined thoroughly in a paper closely related to the present one, in which some of the results for one of the gels involved in the present work have already been reported.[12] The technique allows investigation of the lattice configurations at a nanoscopic level through the determination of the so-called quadrupole parameters that describe the electric-field gradient (EFG) at Zr(Hf) sites. These quantities are the quadrupole frequency ω_Q and the asymmetry parameter η, which can be derived from the fitting of the experimental spin rotation curves $A_2G_2(t)$ obtained at the laboratory. In addition, the relative abundance *f* of each nonequivalent site, the degree of broadening δ of the EFG due to the presence of impurities or defects in the lattice, and the relaxation constant λ related to eventual atomic or defect motions, can be determined by the same procedure. The method has been successfully applied by many authors to the study of the thermal evolution of pure[12] and doped zirconias.[13–15] In some of those works, it has been established that two perfectly distinguishable forms of the metastable tetragonal phase can coexist, in correspondence with an XRD pattern very similar to that of the high-temperature t-ZrO_2 phase. One of them, predominantly present at the lowest temperatures in most tetragonal stabilized zirconias, is the strongly distorted and disordered configuration named t′-form, with the η value above 0.5 and probably oxygen defectively coordinated. In as-obtained materials produced by the sol-gel method, this structure diffracts with very broad signals at the angular positions of the most intense cubic or tetragonal peaks. The other configuration, hereinafter named simply t-form, is the eight oxygen coordinated, slightly distorted ($\eta \leqslant 0.2$ instead of zero), and quite ordered nanostructure that predominates at higher temperatures and exhibits at all temperatures a crystalline tetragonal pattern. The oxygen vacancies movement in doped zirconias and the t′ $\rightarrow$ t transformation between the highly defective and the nearly regular configurations are processes that have been observed in all metastable tetragonal zirconias as the temperature is increased. This experimental evidence proves that a thermally activated redistribution of oxygen vacancies, probably induced by oxygen absorption, takes place.[15] In most zirconias prepared by the sol-gel method starting from an organic precursor, in addition to the previously described tetragonal t′-form, part of the as-obtained amorphous product as revealed in XRD is described by another very disordered configuration of intense EFG, which has been labeled *x*.[12] The disappearance at about the calcination temperature of the organic groups has led to the conclusion that it describes zirconium environments still containing organic residues. Hyperfine quadrupole parameters for the equilibrium phases as well as for the metastable tetragonal forms of zirconia, derived from the experimental PAC spectra or spin rotation curves $A_2G_2(t)$, are well known.[12]

II. EXPERIMENTAL

A. Sample preparation

Two starting solutions were prepared by adding zirconium n-propoxide (ZNP) (70 wt% in 2-propanol, Alfa 22989) to 2-propanol, under an anhydrous nitrogen atmosphere. To one of them, hereinafter called NS, nitric acid was incorporated. The other one was called AS. Subsequently, a mixture of distilled water and acetic acid (3:1 weight ratio) was carefully added to each one of the solutions as it was stirred. The final pH of the solutions was 0.5 for NS and 5.5 for AS. The NS solution was quite transparent and yellow, and the AS precursor was translucent and white. The gel powders were obtained by gelling the solutions in an open flask at 60 °C under normal atmosphere and subsequent heating at 100 °C to achieve a dry residue. Table I lists some characteristics of the sample preparation.

B. Scanning electron microscopy, XRD, and BET measurements

Scanning electron microscopy (SEM) was carried out on the as-obtained gels. XRD patterns were obtained at room temperature for the gels, both as prepared and after heating treatments in normal atmosphere at several temperatures ranging from 100 to 900 °C, the heating rate

TABLE I. Preparation conditions and specific area values for AS and NS zirconia gels.

				Specific area (m^2/g)	
pH	Code	Added acid	Powder color	(As-obtained)	(After 1000 °C annealing)
0.5	NS	Nitric + acetic	Pale yellow	5	3.95
5.5	AS	Acetic	White	340	8.65

being 200 °C/h. After the powder was held for 1 h at the specified temperature, air quenching cooled it. XRD data were collected on a Phillips PW1700 diffractometer of 0.0018° instrumental broadening, using Cu K_α radiation and a graphite monochromator (with a step size of $2\theta = 0.02°$ and at 5 s per step). XRD spectra of the samples were obtained in the $2\theta = 20°$ to 105° diffraction region. The high angle portion $2\theta = 72°$ to 76° was carefully inspected since it allows for a decision between the tetragonal structure through its (004) and (400) reflections and the cubic structure through its unique (400) reflection in between. Powder diffraction spectra were exploited to calculate average crystallite sizes from the magnitude of the half-width of (111) and ($\bar{1}11$) peaks for the tetragonal and monoclinic phases, respectively, by using Scherrer's equation.[16]

Total specific areas were obtained from the BET method using a 2000 E Accosorb Micromeritics instrument. Measurements were performed on samples calcinated for two days at different temperatures up to 1000 °C under normal atmosphere.

C. Thermal analyses

By means of a Netzsche STA 409 analyzer, simultaneous DTA-TGA measurements were carried out on approximately 50 mg of the as-obtained powder gels in normal atmosphere between room temperature and 1350 °C. MgO crucibles and a α-alumina reference were used. The system was calibrated against the melting point of Au (1063 °C). The heating and cooling rates were 10 °C/min. The temperatures of DTA events were determined by the usual method, which uses the intersection of the DTA line base with the extension of the linear region of the rising peak slope. The uncertainty was estimated at ±5 °C.

D. PAC experiment

About 150 mg (≈ 0.025 cm^3) of the powder gels were encapsulated in air at atmospheric pressure in sealed quartz tubes (0.5 cm in diameter and 3 cm long) and then neutron irradiated with a flux of 10^{13} neutrons cm^{-2} s^{-1} for 24 h to achieve the desired activity of ^{181}Hf. The quartz tube was placed inside a small tubular oven (5 cm outer diameter and 0.7 cm inner diameter) whose axis was perpendicular to the plane of the detectors and 4 cm distant from them. The small dimensions of the sample guaranteed the temperature homogeneity throughout it. The hyperfine interaction was determined using a two-CsF detector spectrometer of temporal resolution $\tau_R = 0.75$ ns. The thermal range covered was room temperature to 1050 °C, the mean measurement temperature uncertainty was ±5 °C, and the rate of temperature change between measurements was 120°/min. The PAC spectra $A_2G_2(t)$ obtained at the laboratory were then fitted to a theoretical function by a nonlinear least-squares fitting procedure. The quadrupole parameters depicting the lattice EFGs at hafnium (zirconium) sites were obtained from the best fits achieved.

III. RESULTS

A. SEM, XRD, and BET results

The SEM micrographs in Fig. 1 give evidence of substantial differences between the two gels. While Fig. 1(a) reveals that NS is made up of particles with a mean size of 12 μm and planar faces, AS exhibits the morphology of a very porous material, made up of rounded and small particles about 1 μm in size. The XRD patterns shown in Fig. 2 for the two as-obtained powder gels indicate the presence of amorphous material. After annealing at 850 °C, the predominant structure is monoclinic zirconia, and after annealing at 1000 °C (not shown), only the monoclinic phase is present. However, for intermediate annealing temperatures, appreciable differences between

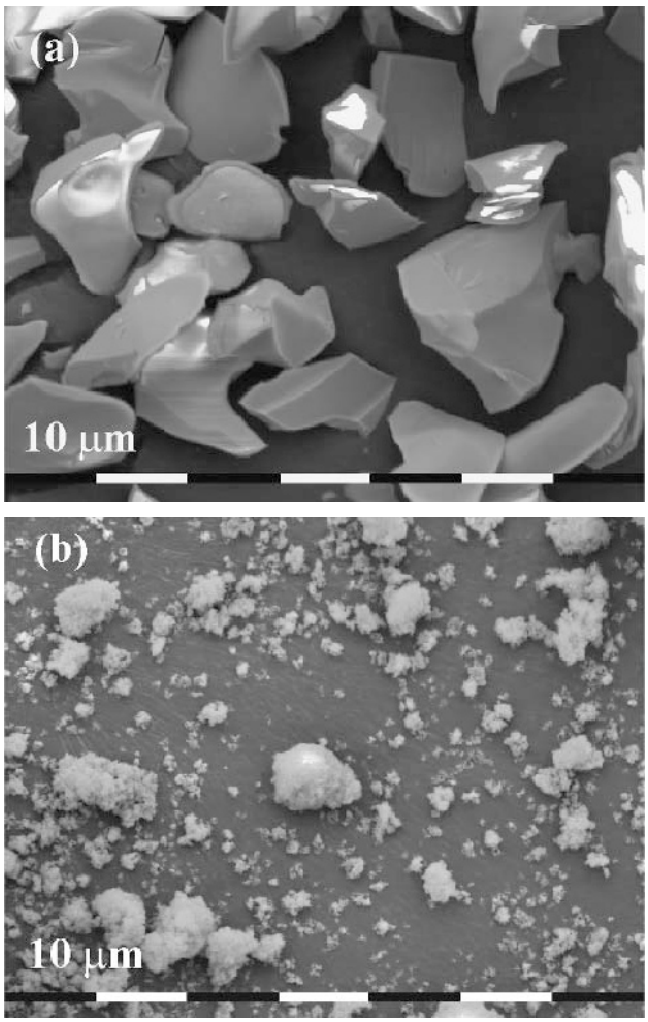

FIG. 1. SEM micrographs of the as-obtained products: (a) NS powder gel and (b) AS powder gel.

the two samples appear. AS exhibits well-defined tetragonal peaks and traces of monoclinic phase after annealing at 250 °C and increasing amounts of the latter phase for higher annealing temperatures. On the other hand, NS reveals the crystallization of the tetragonal phase after annealing at 350 °C and the appearance of traces of monoclinic zirconia for annealing temperatures not below 450 °C. The high angle diffraction region (see the magnification in NS at 500 °C) allowed the identification of tetragonal stabilized zirconia.

Available XRD-derived mean tetragonal crystallite sizes in Fig. 3 show that the values for NS are greater than those for AS and also show a different thermal behavior for the samples. Table I reveals that the specific surface area value for the as-obtained NS gel is about 70 times smaller than the corresponding one for AS. The crystallite size of NS increases approximately 20%, and the surface area decreases almost the same amount over the thermal ranges investigated, indicating that the sample does not suffer substantial morphological changes. On the contrary, both magnitudes show more drastic changes in AS, the crystallite size undergoing a relevant increase above 350 °C and the specific surface exhibiting a continuous and significant decrease as the sample is heated at increasing temperatures (see Table I and also the normalized specific surface in Fig. 4). The monoclinic crystallite sizes after annealing at 850 °C (not plotted) are similar in the two samples, having grown to about 32 nm. Accordingly, after the 1000 °C treatment, the specific area values become lower and similar.

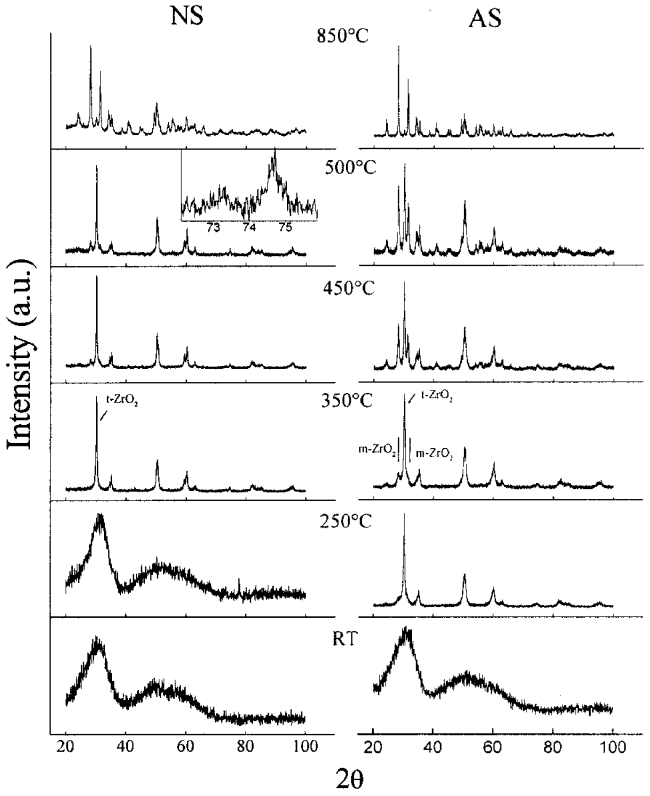

FIG. 2. Selected XRD patterns of the as-obtained powder gels and after 1 h annealing at the temperatures indicated. The inset in NS at 500 °C corresponds to the (004) and (400) reflections of tetragonal zirconia.

B. TGA-DTA results

The bulk thermal behavior for NS and AS plotted in Fig. 5 indicates a quite dissimilar gel–ceramic conversion. It is clear that, compared with NS, AS exhibits a

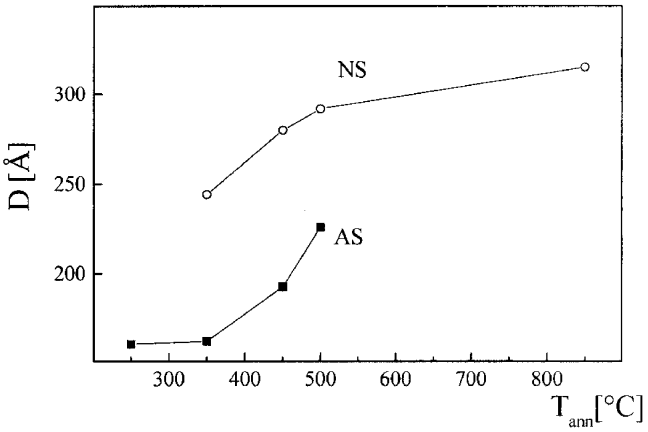

FIG. 3. Thermal evolution of mean tetragonal crystallite size derived from XRD data.

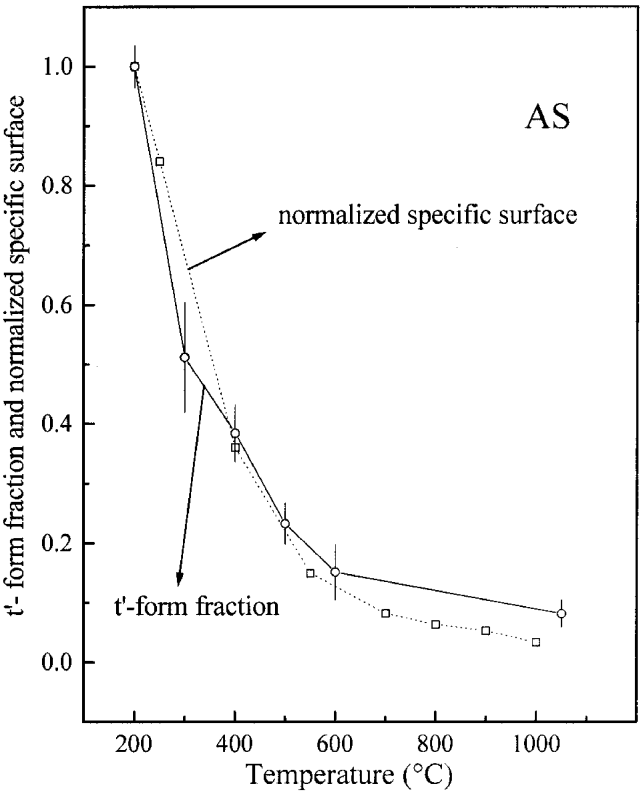

FIG. 4. Thermal evolution of the t′-form fraction and normalized specific surface for AS sample.

somewhat smaller total mass loss and DTA changes occur in a narrower thermal range and end at a much lower temperature.

1. NS sample

This gel exhibits TGA-DTA curves (Fig. 5) very similar to those reported for other ZrO_2-based gels obtained in similar conditions.[12] Hence, the identification of the thermal changes made there has been also assumed in this work. TGA data for NS (top of Fig. 5) indicates a continuous (beginning at 100 °C) and drastic (from near 200 °C) loss of mass up to 400 °C. Above this temperature and up to near 580 °C there is a last, very pronounced mass loss, reaching the highest rate at 470 °C. Finally, at approximately 600 °C, a subtle change in the slope of the curve appears, followed by a weak mass gain over the region 600–1000 °C (see the detail at the right top), as was also observed in other sol-gel-derived tetragonal zirconias, i.e., pure ones prepared using solvents other than 2-propanol[12] as well as yttria-doped ones.[15] Regarding the DTA results plotted in Fig. 5, the onset of each thermal event is always closely correlated with the mass changes reported. The curve shows subtle slope changes at low temperatures known to correspond to the elimination of adsorbed water and solvent. In the range 250–350 °C, a double and broad peak identifying bound water and organic residues elimination can be seen. At higher temperatures, the well-defined, large and asymmetric exothermic peak attributed to dehydroxylation appears at 495 °C. However, this peak has also been interpreted as the onset of phenomena related to the structure evolution, i.e., the oxide crystallization.[12,15] The very wide peak starting over 600 °C and centered at 790 °C, in correspondence with the last changes observed in the TGA curve, is known to correspond to the elimination of the last $(OH)^-$ groups, oxygen absorption, and the progression of structural changes.[12]

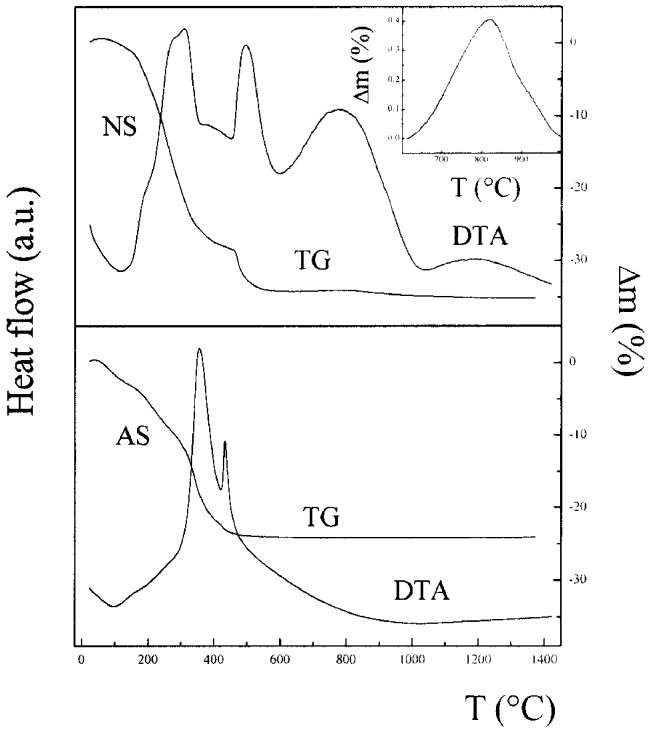

FIG. 5. DTA-TG heating curves taken at 10 °C/min. The detail corresponds to the thermal range of oxygen absorption in the NS sample.

2. AS sample

TGA data of Fig. 5 (bottom) indicate a continuous loss of mass beginning at room temperature and ending near 470 °C. A detailed analysis of this curve makes it possible to distinguish three thermal regions of increasing slopes, centered at around 100, 220, and 370 °C and a fourth one that gives evidence of a small mass loss near 450 °C. The first change can be interpreted unambiguously as water loss. In turn, the DTA curve shows subtle changes below 300 °C and well-defined exothermic peaks at 355 and 450 °C.

C. PAC results: Structure at nanometer scale

Figure 6 shows selected PAC spectra along with the best-fitting curves and gives evidence of the dissimilar thermal behavior of the hyperfine interaction determined in the two samples investigated. Detailed information derived from the fits of the PAC spectra is contained in Fig. 7 and is described in the following.

1. NS sample

(i) The as-obtained gel consists entirely of the highly disordered *x*-form representing zirconium environments still containing organic residues, and this situation is unaltered up to 250 °C. (ii) Between 450 and 550 °C the interactions corresponding to the metastable tetragonal phase, i.e., the distorted and disordered t′-form and the nearly regular and ordered t-form fully describe the material. (iii) At 550 °C, a sudden increase of the broadening of the t′-phase suggests the unresolved presence of some other Zr site. Accordingly, at 650 °C, monoclinic zirconia erupts at the expense of the tetragonal t′-form and achieves 90% relative abundance at 1050 °C. (iv) Regarding the thermal evolution of the hyperfine parameters, it can be observed that the quadrupole frequency of the t′-phase shows a continuous decrease, very pronounced over the 450–650 °C range.

2. AS sample

(i) At room temperature both the t′-form and *x* are present, though the intensity of the latter one is very weak. A large broadening (about 40%), commonly due to either a highly inhomogeneous material or to the existence of an additional unresolved site, characterizes the

major t′-form describing the as-obtained product. This situation probably yields values for the corresponding quadrupole frequency and asymmetry parameter quite out of the tendency they display at higher temperatures. (ii) At 200 °C the disappearance of x has given rise to an increase of t′ phase and to the appearance of the monoclinic phase, somewhat distorted. Along with the eruption of the new structure, the t′ phase broadening diminishes, and the fitted parameters of its EFG become more reliable. (iii) From 200 °C on, the quadrupole frequency of the t′-phase shows a drastic reduction up to 400 °C and the asymmetry parameter, a continuous increase up to the highest temperatures. (iv) At 300 °C the monoclinic phase shows its proper hyperfine features; it continually grows at the expense of the t′-form and achieves 90% of relative abundance at 600 °C. (v) At 1050 °C the monoclinic to tetragonal equilibrium phase transition has partially occurred, the powder becoming nearly half tetragonal. Figure 4 shows the thermal evolution of the t′–PAC relative abundance along with that of normalized specific area for the AS gel.

IV. DISCUSSION

Regarding as-obtained gels, both of them appear amorphous to XRD but show apparent differences when investigated by other techniques. One difference, manifested at a nanoscopic scale (see Fig. 7), is that AS is predominantly described by the distorted tetragonal t′-form and in a minor proportion by the *x*-form, while NS is described entirely by the last interaction. Recalling that the t′-form originates from hydrolyzed species,[12] the starting population ratio t′/*x* between the two highly disordered forms could give some insight into the degree of hydrolysis achieved during synthesis. This ratio, valued at 3 and 0 for AS and NS, respectively, shows that the extent of hydrolysis decreases drastically when the pH of the precursor solution is reduced from 5.5 (AS) to 0.5 (NS). Another difference is the extremely porous aspect of AS (see Fig. 1), in coincidence with surface area about two orders of magnitude larger than that of NS (see Table I). Both descriptions of the less acidified AS sample, morphological and nanoscopic, match coherently: the predominant t′-form involving defective atomic arrays can adequately provide the numerous surfaces of this porous material.

On the other hand, the morphology of the NS powder along with its smaller specific surface indicates that the extent of condensation is also affected by the pH of

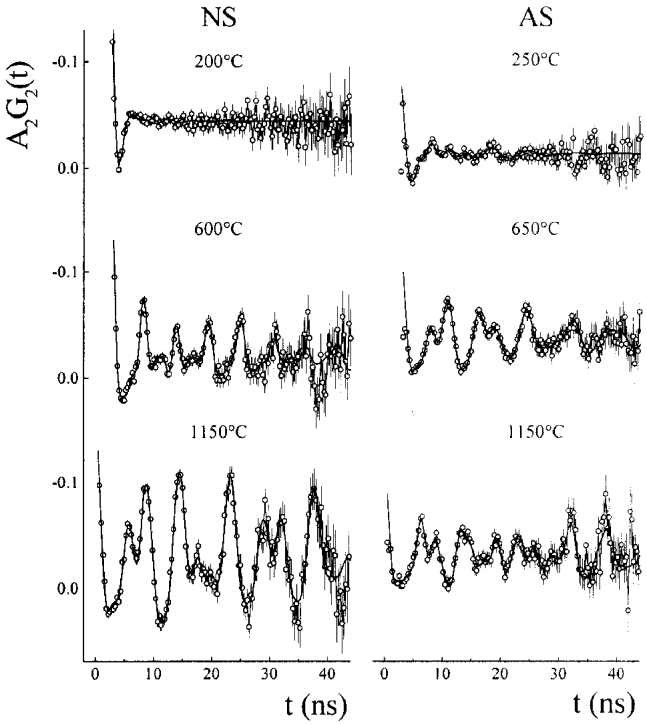

FIG. 6. Selected PAC spectra. Measurement temperatures are indicated. Full lines correspond to the best fitting curves.

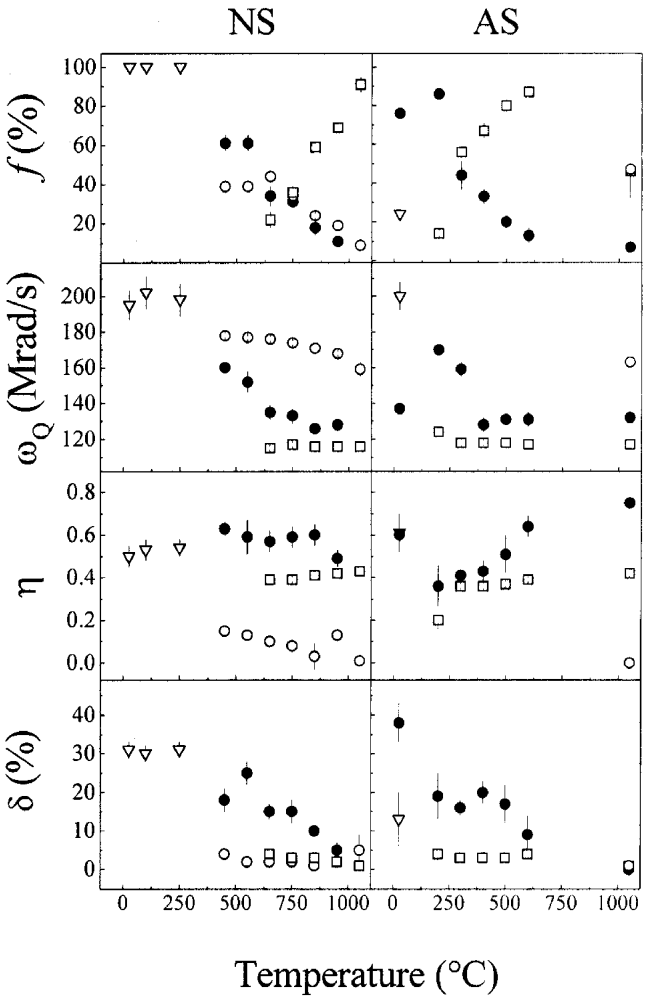

FIG. 7. Thermal evolution of PAC relative fractions and quadrupole parameters: (▽) *x*, (●) t′, (○) t, and (□) m-ZrO_2.

the precursor solution. In fact, it seems that the lower the pH, though the degree of hydrolysis is lower, the easier it is for the condensation reaction to give larger species that still involve organic groups. These experimental results can be explained by assuming that the hydrolysis reaction in ZNP occurs via the nucleophilic attack of zirconium ions and also of the $(RO)^-$ groups during solvatation[8] by the $(OH)^-$ groups. A reduction in pH will lead to a protonation of the nucleophilic agent, thus decreasing its reactivity and the degree of hydrolysis and promoting condensation reactions that lead to larger species.[5] A higher pH, on the other hand, will assist the formation of branched chains leading to species containing superficial $(OH)^-$ groups.

Despite the different thermal treatments involved in XRD, DTA-TGA, and PAC measurements, a correlation between bulk thermal events and the evolution of nanoscopic zirconium environments proved by the hyperfine experiments could be established.

In NS, the presence of the unique *x*-form up to 250 °C (Fig. 7) matches the TGA-DTA outstanding change observed between 250–350 °C (Fig. 5) partially assigned to organic residues elimination. The XRD visualization (Fig. 2) of the tetragonal and monoclinic phases after heating respectively at 350 and 850 °C (it must be pointed out that there were no heating treatments at temperatures between 500 and 850 °C) correlates fairly well with the PAC detection of the tetragonal phase in its two t′- and t-forms at 450 °C and the occurrence of the monoclinic phase at 650 °C on. The temperatures of these two structural transformations also match the TGA-DTA changes observed around 480 °C and in the region 600–1000 °C. Recalling that these two signals were partially assigned to the removal of hydroxyl groups, the authors assumed that the first one corresponds to easily removable superficial groups and the last one to more linked groups localized in the bulk. From the thermal variations observed in the quadrupole frequency describing the distorted t′-configurations and, contrarily, the smooth thermal evolution of the parameters that describe the m-phase and the t-form at all temperatures (Fig. 7), it has been inferred that only the t-form zirconium environments change substantially as hydroxyl removal takes place. Consequently, it seems reasonable to conclude—as expected—that it is the defective t′-configuration that trapped the hydroxyl groups. Furthermore, the different decrease of the quadrupole frequency, relevant within the 450–650 °C and moderate at higher temperatures, seems in agreement with the hydroxyl groups removal as a two-step process. Supporting these considerations, it must be realized that in sol-gel-derived zirconias, defective Zr^{4+} surroundings can result from the localization of zirconium ions near defect sources (dislocations, grain boundaries, or particle surfaces) and also from the occupation of a nearby oxygen site by a preparation-derived residual group or the vacancy that the latter leaves when it is thermally removed. It can thus be recognized that hydroxyl elimination from the bulk, far from any oxygen source, must likely leave a nonstoichiometric, oxygen defective, and thermodynamically unstable structure. Provided oxygen diffusion becomes operative, atmospheric oxygen is incorporated and zirconia destabilization occurs via the tetragonal-to-monoclinic phase transformation. Confirming the last hypothesis, it has been reported that monoclinic phase crystallization is favored by the oxygen absorption that takes place once the last $(OH)^-$ groups have been eliminated.[4]

In AS, PAC results in Fig. 7 indicate that the transformation between the two disordered configurations *x* and t′-form occurred below 200 °C and allowed the assignment of the mass loss centered at 220 °C to the early elimination of organic groups. Assisted by the association between DTA-TGA information and nanoscopic thermal changes made for the NS gel, the authors have assigned the sharp DTA peak at 355 °C and relevant mass loss centered at 370 °C to the elimination of $(OH)^-$ groups involved in the t′-configurations. The identification matches the assumption that most hydroxyls in AS are located on the surfaces, thus being easily removed, and justify the pronounced reduction observed in the t′-form quadrupole frequency over the corresponding thermal region. The same DTA event must also be associated with the crystallization of the tetragonal phase, according to the x-ray diffractogram obtained after heating at 250 °C and the reduction in the δ disorder parameter of the t′-configurations at 200 °C. The appearance and subsequent crystallization of the monoclinic phase at the expense of the t′-atomic arrays observed by PAC are in complete correspondence with the XRD patterns obtained after heating at 250 and 450 °C, respectively. So, the last DTA peak at 450 °C is interpreted as the monoclinic phase crystallization and the corresponding last and small mass loss is associated with the simultaneous elimination of the last remaining hydroxyls. It is worth pointing out the absence of the regular t-form over the whole thermal range investigated. The mass gain attributed in NS to oxygen absorption was not detected in this sample. Its absence could be understood assuming that this process occurs simultaneously with hydroxyl removal, a predominantly superficial process in the case of AS. The similarity between the behaviors of the fraction of the t′-form and of the normalized specific surface area shown in Fig. 4 is further proof that the atomic configurations at the surfaces of the highly porous material are described by the t′-form. As temperature increases, the pores collapse, and the porosity is reduced. This effect is evidenced at a nanoscopic level through the conversion of the t′-form to the monoclinic phase. In turn, the thermal behavior of the asymmetry parameter η of the

t′-form reflects an unusual increasing distortion of these tetragonal defective configurations. This is an unexpected result, considering the fact that any specific atomic configuration tends to increase its symmetry as temperature is increased. However, it can be realized that as the defective sites mostly localized at the surfaces are subjected to an increasing stress as the pores' radii reduce, an enhanced distortion becomes possible. This experimental evidence had already been observed in a tetragonal zirconia thin film[15] and explained as due to the stresses developed by the film–substrate linkage.

It was determined that the less-acidified gel is the one that most easily transforms to the monoclinic phase. The comparison between the crystallite sizes exhibited by AS and NS (Fig. 3) seems to indicate that in the present investigation the stability of the metastable tetragonal phase is not determined only by a size factor as has been often reported, but that it could as well be related to the localization of the $(OH)^-$ containing t′ defective atomic configurations in the lattice. In fact, the superficial position of these configurations in AS makes easier hydroxyl removal and concomitant oxygen absorption, thus causing the destabilization of metastable tetragonal towards monoclinic zirconia at an early temperature.

V. CONCLUSIONS

The PAC technique was applied to the study of two sol-gel-derived zirconia powders coming from precursor solutions with very low pH and medium pH, respectively. The hyperfine method proved efficient for a nanoscale interpretation of the differences found in the morphology and structure of the gels as determined by SEM, XRD, and DTA-TGA.

In the as-prepared powder gel of precursor solution of pH = 0.5, the hydrolysis extent of the derived gel was low, and a more condensed species still containing organic groups was obtained in comparison with the powder gel coming from precursor solution of higher pH. Once the organics were calcinated though, the material came to be described by the two known tetragonal nanoconfigurations around Zr^{4+} sites, only the strongly distorted and disordered ones of the t′- phase evidenced changes in the quadrupole parameters as hydroxyl groups were eliminated with temperature. The removal of the hydroxyl groups at the surface corresponded with the crystallization of the tetragonal phase near 450 °C. In turn, the elimination of the hydroxyl groups localized at the bulk took place at a higher temperature, leaving an excess defective structure. When the diffusion mechanisms became operative, oxygen vacancies healing caused by oxygen absorption from the atmosphere occurred and the monoclinic phase erupted.

At pH = 5.5, a very porous material of very large specific surface area and highly hydrolyzed corresponded with a predominant content of strongly distorted and disordered t′ tetragonal configurations. As temperature increased, the thermal evolution of the residual porosity matched fairly well the decreasing relative abundance of the t′-phase, and the superficial localization of this latter was reflected by an enhanced distortion of the corresponding nanoconfigurations around Zr^{4+} sites. This situation favored the low temperature removal of hydroxyls and the early appearance of the monoclinic phase.

The comparison between the two samples differing in the pH of the precursor solution allowed for the conclusion that the localization of the defective $(OH)^-$ containing Zr^{4+} surroundings plays an important role in the stabilization of the metastable tetragonal phase.

ACKNOWLEDGMENTS

Financial support provided by Comisión de Investigaciones Científicas de la Provincia de Buenos Aires (CICPBA) and Consejo Nacional de Investigaciones Científicas y Técnicas (CONICET) is gratefully acknowledged.

REFERENCES

1. R.C. Garvie, J. Phys. Chem. **82,** 218 (1978).
2. F. Wu and S. Yu, J. Mater. Sci. **25,** 970 (1990).
3. P. Kountouros and G. Petzow, in *Science and Technology of Zirconia V,* edited by S.P.S. Baldwal, M.J. Bannister, and R.H.J. Hannink (Technomic Publishing Company, Lancaster, PA, 1993), p. 30.
4. R. Gómez, T. López, X. Bokhimi, E. Muñoz, J.L. Boldú, and O. Novaro, J. Sol-Gel Sci. Technol. **11,** 309 (1988).
5. C. Stöcker and A. Baiker, J. Non-Cryst. Solids. **223,** 165 (1998).
6. B.E. Yoldas, J. Mater. Sci. **21,** 1080 (1986).
7. M. Nabavi, S. Doeuff, C. Sanchez, and J. Livage, J. Non Cryst. Solids. **121,** 31 (1990).
8. C. Sanchez, J. Livage, M. Henry, and F. Babonneau, J. Non Cryst. Solids. **100,** 65 (1988).
9. R. Srinivasan, M. Harris, S.F. Simpson, R.J. De Angelis, and B.H. Burtron, J. Mater. Res. **3,** 787 (1988).
10. B.H. Davis, J. Am. Ceram. Soc. **67,** C168 (1984).
11. J.C. Debsikdar, J. Non Cryst. Solids. **87,** 343 (1986).
12. M.C. Caracoche, P.C. Rivas, R. Caruso, E. Benavídez, O. de Sanctis, M.M. Cervera, and M.E. Escobar, J. Am. Ceram. Soc. **83,** 377 (2000).
13. A. Baudry, P. Boyer, and A.L. de Oliveira, Hyperfine Interactions. **10,** 1003 (1981).
14. J.A. Gardner, H. Jaeger, H.T. Su, W.H. Warnes, and J.C. Haygarth, Physica **B150,** 223 (1988).
15. R. Caruso, E. Benavídez, O. de Sanctis, M.C. Caracoche, P.C. Rivas, M.M. Cervera, A. Caneiro, and A. Serquis, J. Mater. Res. **12,** 2594 (1997).
16. H.P. Klug and L.E. Alexander, *X-Ray Diffraction Procedures for Polycrystalline and Amorphous Materials* (John Wiley and Sons, New York, 1974), Ch. 9.